

Acceptance of low- Q^2 tagger

Jaroslav Adam
October 27, 2020

Abstract

Acceptance of forward electron tagging is given as a function of several kinematics variables. The results are compared between two event generators. The first section introduces the event generators along with characteristics of generated events. Geant4 model is described in the second section. The results are shown in the third section.

Contents

1	Generated samples	1
1.1	Angular divergence and vertex spread	1
1.2	Pythia6	1
1.3	Quasi-real (QR) photoproduction	1
1.4	Total cross section as a function of Q^2	2
1.5	Properties of generated samples	3
1.6	Effect of beam angular divergence	7
2	Geant4 model	9
3	Results on the acceptance	10
3.1	Acceptance in a single variable	10
3.2	Acceptance in two variables	14
4	Summary	18
A	Generator steering cards	19
A.1	Pythia6 card	19
A.2	Quasi-real card	21
B	Steering cards for lmon geometry	22
B.1	Top geometry	22
B.2	Tagger detectors geometry	22
B.3	Beamline layout	22

1 Generated samples

Two samples of scattered electrons, Pythia6 and quasi-real photoproduction, were used for the acceptance. Both samples have 5M events at 18×276 GeV beams. Effects of beam angular divergence and vertex spread were applied to scattered electrons in both samples

1.1 Angular divergence and vertex spread

Smearing by Gaussian rotations in horizontal and vertical directions has been applied to electron 3-momentum in order to implement beam angular divergence. Position at which the scattered electron has been generated was obtained from a set of three Gaussians to account for vertex spread. Details of the procedure are given in ¹ on page 25

1.2 Pythia6

Implementation for ep, the pythiaRHIC ² has been used. Steering card is located in

```
/afs/rhic.bnl.gov/eic/PACKAGES/PYTHIA-RAD-CORR-32BIT/input.data.ep_noradcor.18x275.eic.FF.used
```

the output is in

```
/eicdata/eic0009/PYTHIA/ep/TXTFILES/pythia.ep.18x275.5Mevents.1.RadCor=0.Q2.all.txt
```

and the log is

```
/eicdata/eic0009/PYTHIA/ep/LOGFILES/pythia.ep.18x275.5Mevents.1.RadCor=0.Q2.all.log
```

Full steering card is given in Appendix A.1.

Total cross section is $54.7 \mu\text{b}$.

Event sample of scattered electrons with beam effects applied according to Section 1.1 is located in

```
/gpfs/mnt/gpfs02/eic/jadam/GETaLM_data/py/pythia_ep_18x275_Q2all_beff2_5Mevt.root
```

This will be the Pythia6 input to Geant4 model for the acceptance.

1.3 Quasi-real (QR) photoproduction

The model is based on a low- Q^2 approximation with Regge fit to the total photon-proton cross section. Description is given in ³ on page 23.

Event generator for quasi-real photoproduction is a part of GETaLM generator ⁴ which implements also beam effects in Section 1.1. This particular implementation of beam effects was also used for Pythia6 sample.

Steering card for GETaLM quasi-real photoproduction is located in

¹https://indico.bnl.gov/event/8746/contributions/38747/attachments/28859/44620/JA-Luminosity_and_tagger_20200618.pdf

²<https://eic.github.io/software/pythia6.html>

³https://indico.bnl.gov/event/8746/contributions/38747/attachments/28859/44620/JA-Luminosity_and_tagger_20200618.pdf

⁴<https://github.com/adamjaro/GETaLM>

/gpfs/mnt/gpfs02/eic/jadam/GETaLM_data/qr/quasireal.ini

output is in

/gpfs/mnt/gpfs02/eic/jadam/GETaLM_data/qr/qr_18x275_Qe_beff2_5Mevt.root

and the log is

/gpfs/mnt/gpfs02/eic/jadam/GETaLM_data/qr/qr_18x275_Qe_beff2_5Mevt.log

Full steering card for quasi-real sample is given in Appendix A.2.

Total cross section of quasi-real sample is $54.8 \mu\text{b}$, in good agreement with Pythia8 cross section in Section 1.2.

The quasi-real photoproduction will be abbreviated to QR in the following text.

1.4 Total cross section as a function of Q^2

The cross section in Q^2 , in terms of $\log_{10} Q^2$ is shown in Figure 1 for both samples at the top energy $18 \times 275 \text{ GeV}$.

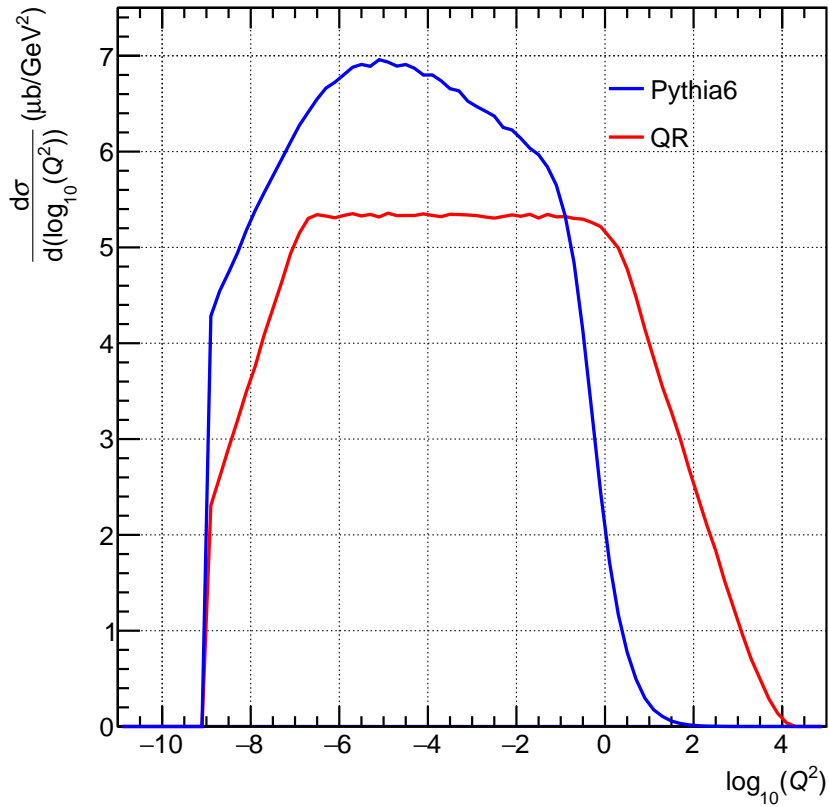


Fig. 1 Total cross section as a function of Q^2 by Pythia6 and quasi-real photoproduction (QR) at $18 \times 275 \text{ GeV}$.

1.5 Properties of generated samples

Generator true event variables and electron kinematics is shown here for both models, Pythia6 and quasi-real photoproduction. The *true* stands for the stage right after event generation, before the beam effects of angular divergence and vertex spread were applied.

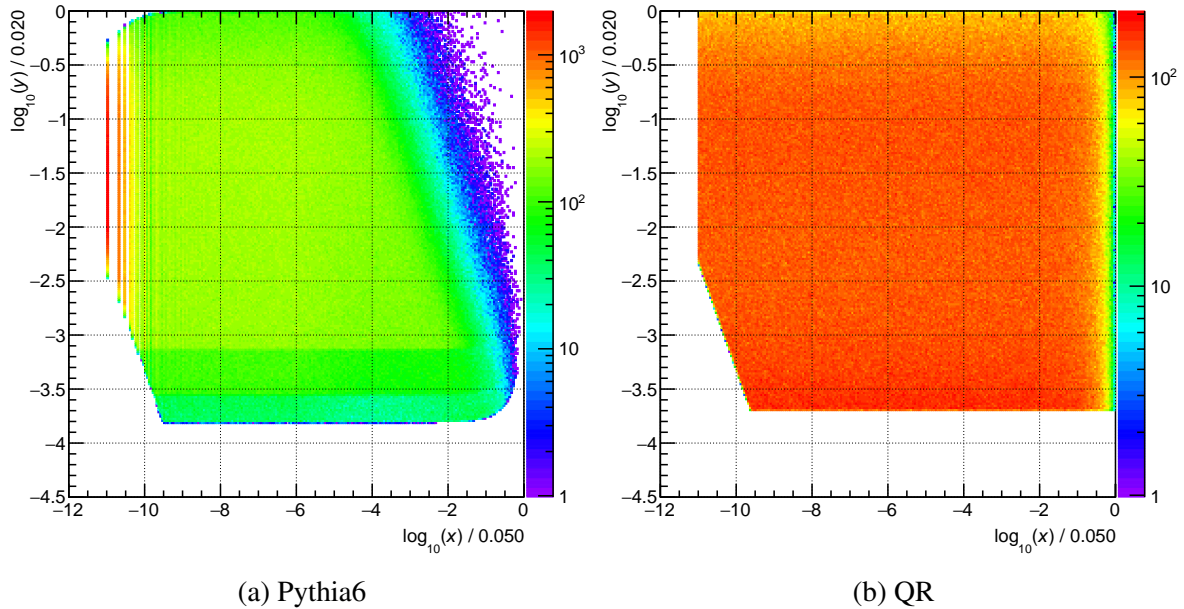
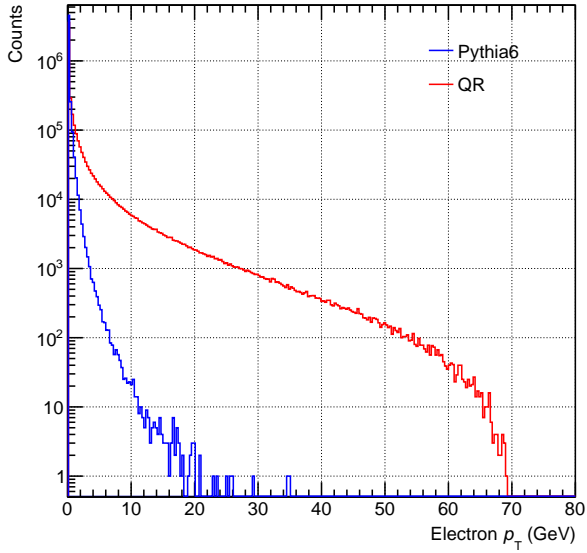
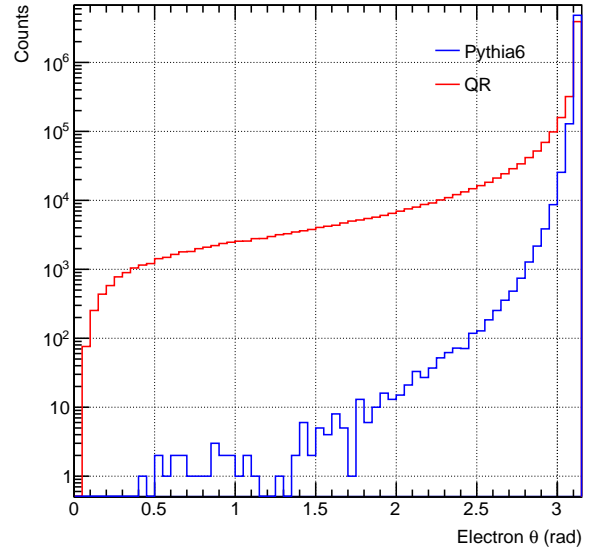
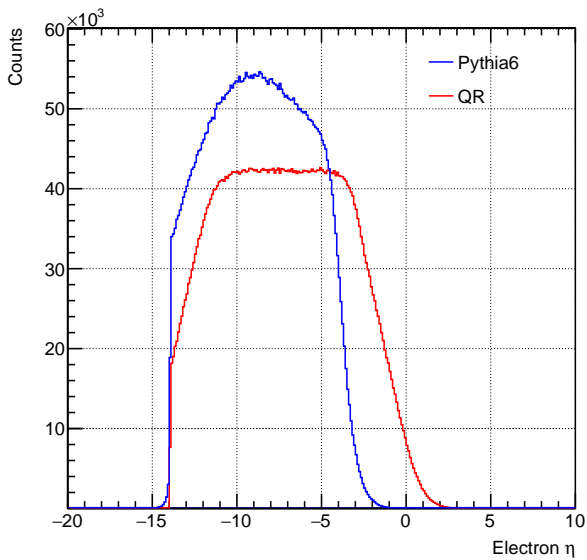
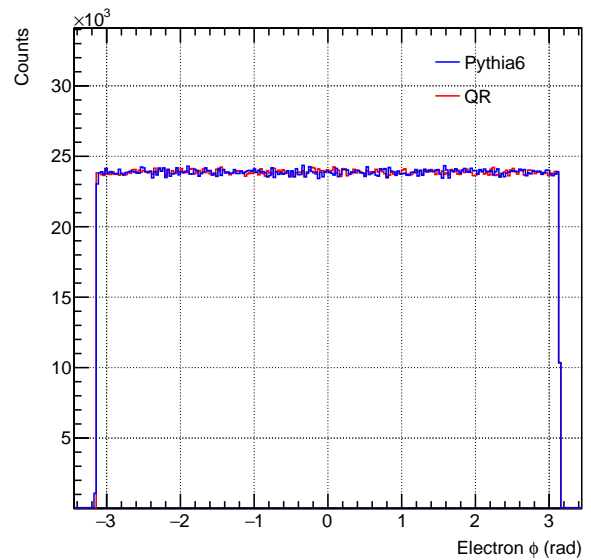


Fig. 2 Bjorken- x and inelasticity y for Pythia6 (a) and QR (b). Structure of lines at large negative x in Pythia6 sample is an artifact of limited numerical precision in its ASCII output.

Fig. 3 Electron transverse momentum p_T .Fig. 4 Electron polar angle θ .Fig. 5 Electron pseudorapidity η .Fig. 6 Electron azimuthal angle ϕ .

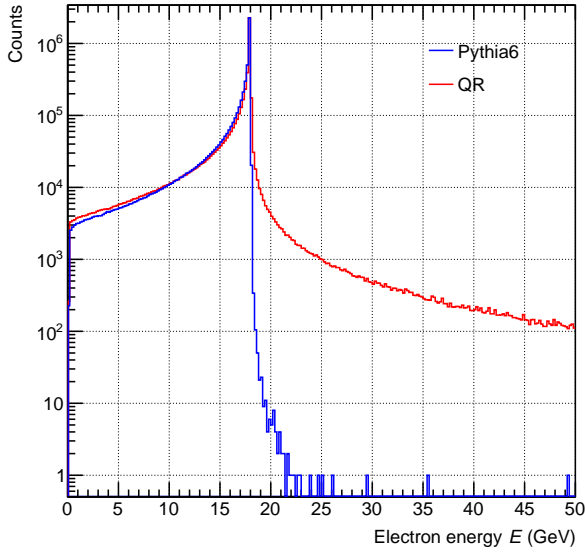


Fig. 7 Electron energy E (GeV).

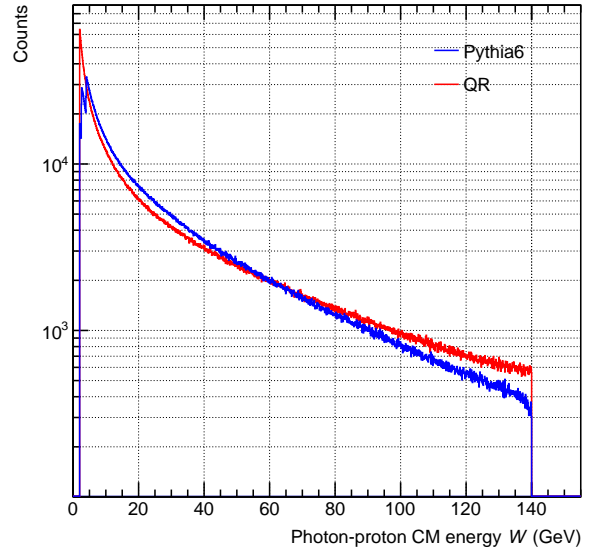
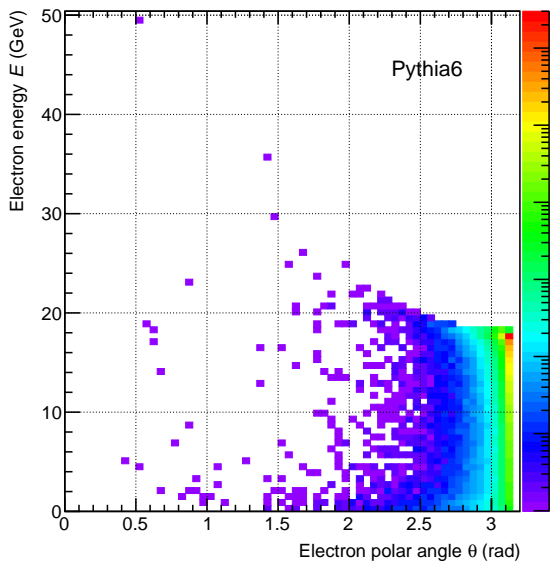
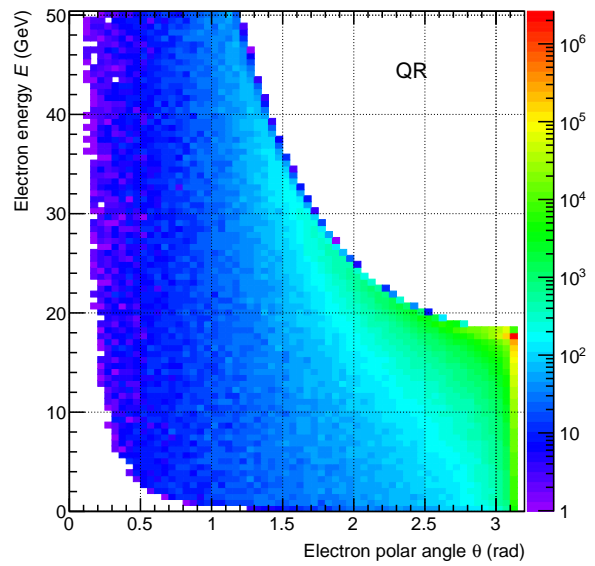


Fig. 8 Photon-proton CM energy W (GeV).



(a) Pythia6



(b) QR

Fig. 9 Electron energy E and polar angle θ for Pythia6 (a) and QR (b).

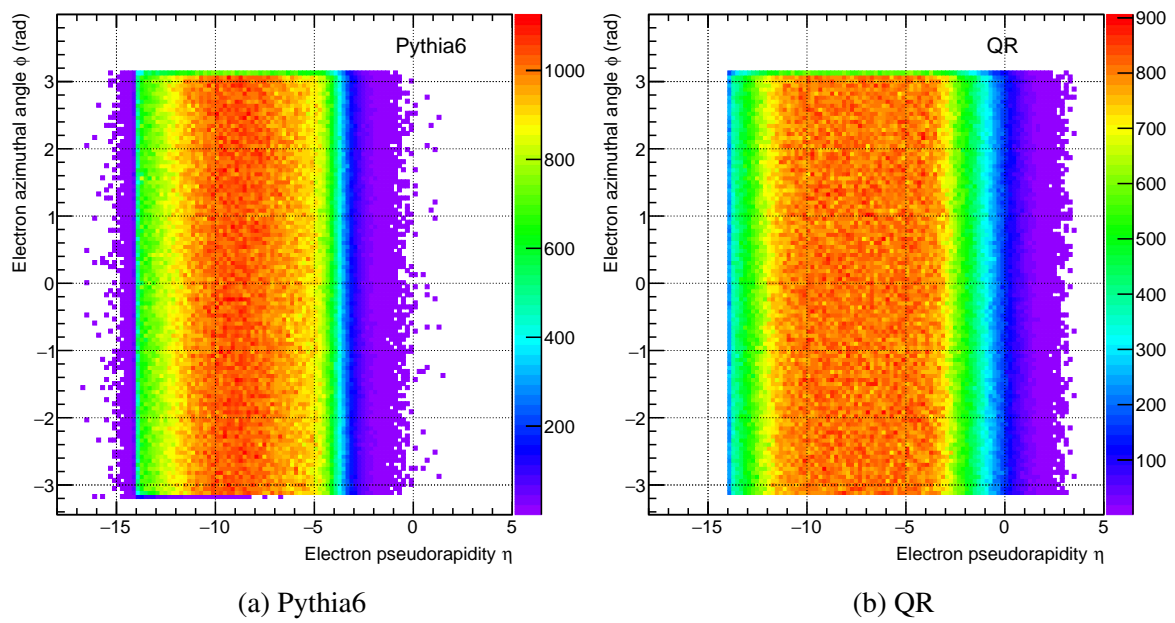


Fig. 10 Electron ϕ and η for Pythia6 (a) and QR (b).

1.6 Effect of beam angular divergence

The divergence alters angular distribution of scattered electrons at small angles. It is seen as modification to polar angles in Fig. 11 ($\theta = \pi$ is direction of electron beam), where a comparison is made between distribution of true generated polar angles and angular distribution after the angular divergence was applied.

A modulation is introduced to originally uniform azimuthal angles, as seen in Fig. 12.

More dramatic behavior is seen in pseudorapidity, Fig. 13. At very small negative η the shape is completely dominated by effect of divergence.

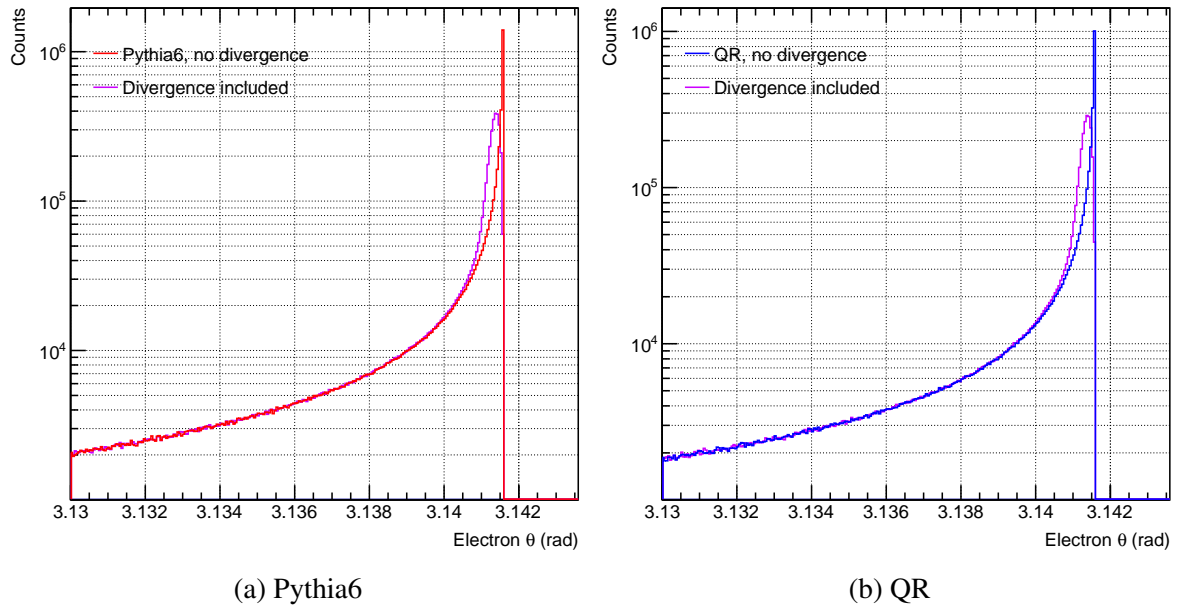


Fig. 11 Presence of angular divergence in polar angle θ for Pythia6 (a) and QR (b).

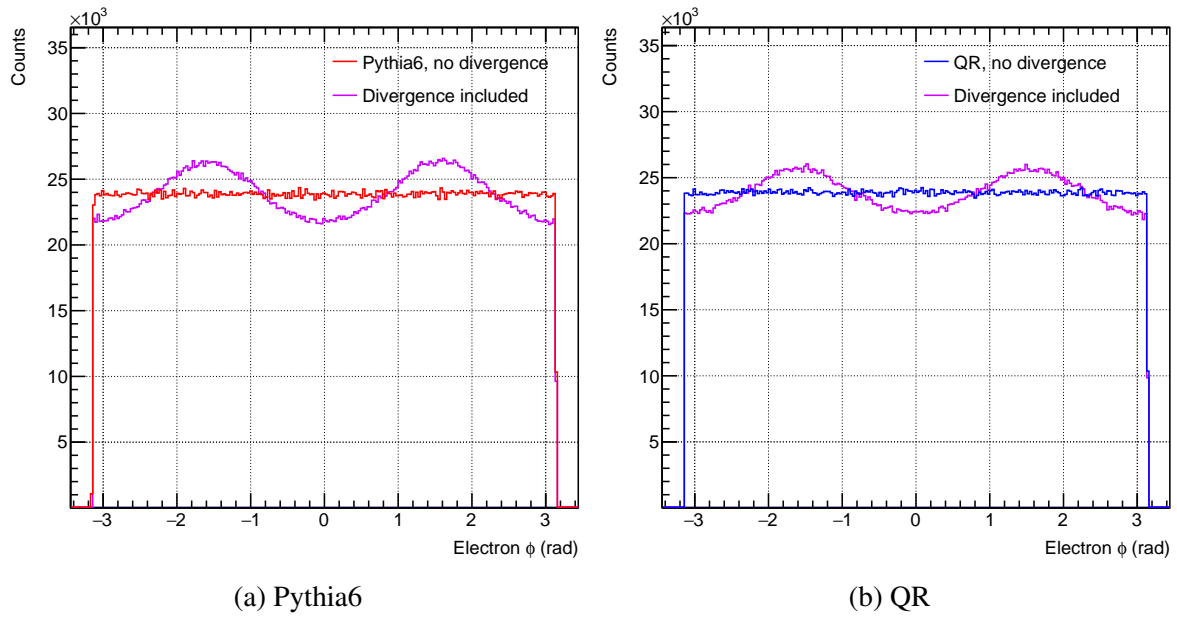


Fig. 12 Presence of angular divergence in azimuthal angle ϕ for Pythia6 (a) and QR (b).

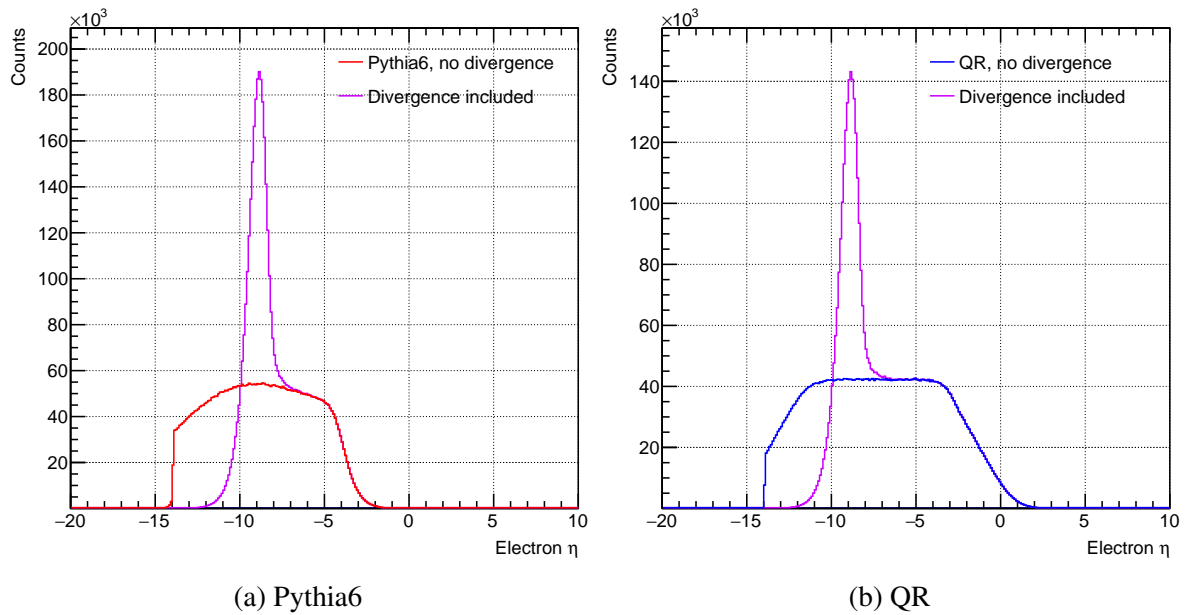


Fig. 13 Presence of angular divergence in pseudorapidity η for Pythia6 (a) and QR (b).

2 Geant4 model

Two tagger detectors are considered along the drift space between B2eR and Q3eR magnets in the electron outgoing side. Details are given in ⁵ on pages 6 and 18.

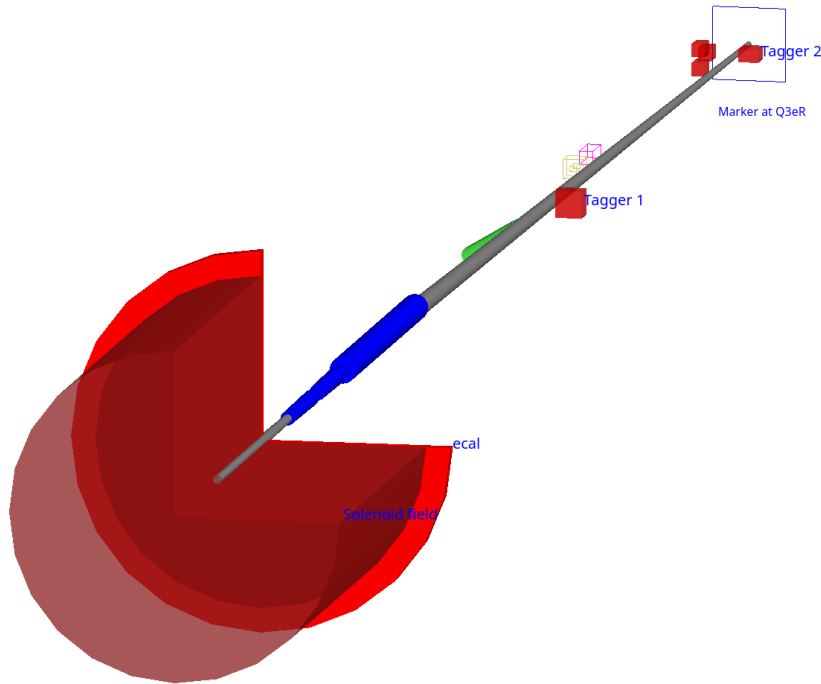


Fig. 14 Geant4 model of electron outgoing IR.

The model is shown on Fig. 14. Tagger 1 is placed at $z = -24$ m, Tagger 2 is placed at $z = -37$ m. Drift space in gray is shown only for visualization, it is transparent to all particles.

Implementation is done as part of lmon package ⁶ originally created for luminosity monitor (the lmon stands for luminosity monitor). Individual beam magnets are implemented using particular Geant4 classes for dipole and quadrupole magnets. The tagger detectors are represented as a boxes of expected calorimeter dimensions which count particles hitting their volume. Energy and position of hit for each track is stored to make also for position sensitive layer in front of the calorimeter.

Full steering cards to define the geometry layout are given in Appendix B.

Input to lmon Geant4 simulation is scattered electrons from one of the generated samples in Section 1 which include beam effects of angular divergence and vertex spread. The output is an array of hits reported by the models of tagger detectors. Also the true event variables and electron kinematics from the point before the beam effects were applied are propagated to lmon output.

⁵https://indico.bnl.gov/event/8742/contributions/38722/attachments/28757/44422/JA-Low_Q2_tagger_20200615.pdf

⁶<https://github.com/adamjaro/lmon>

3 Results on the acceptance

Acceptance for Tagger 1 and Tagger 2 is obtained as a ratio of all generated events to events where the electron makes a hit in one of the taggers. All the acceptance plots were produced with `plots_kine_acc.py`⁷ macro.

3.1 Acceptance in a single variable

Ratio of events with a hit in one of the taggers is constructed in bins of the particular kinematics variable, leaving full range of all the other variables. At regions of limited statistics the bins are automatically made longer to satisfy an upper limit on binomial error in each bin.

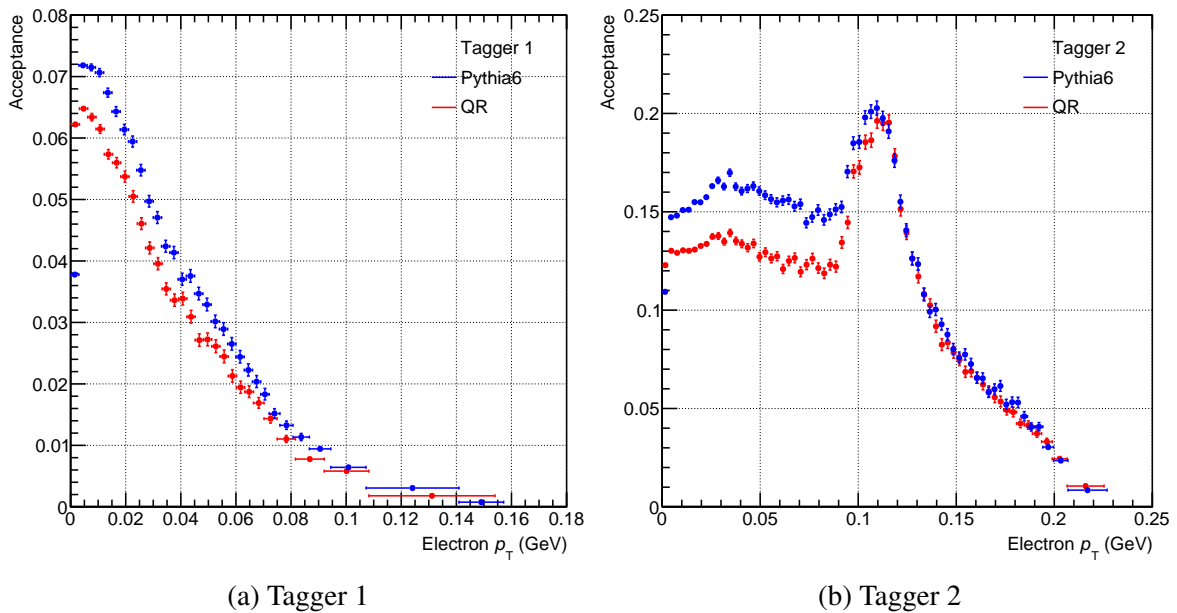


Fig. 15 Acceptance in electron transverse momentum p_T for Tagger 1 (a) and Tagger 2 (b).

⁷https://github.com/adamjaro/Imon/blob/master/macro/plots_kine_acc.py

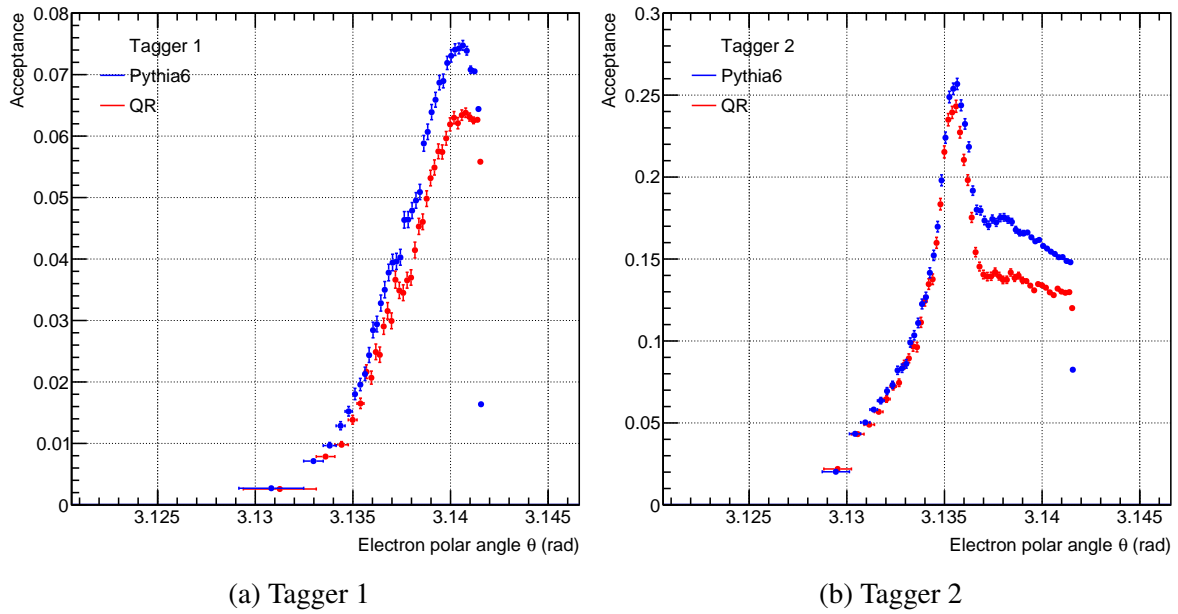


Fig. 16 Acceptance in electron polar angle θ for Tagger 1 (a) and Tagger 2 (b).

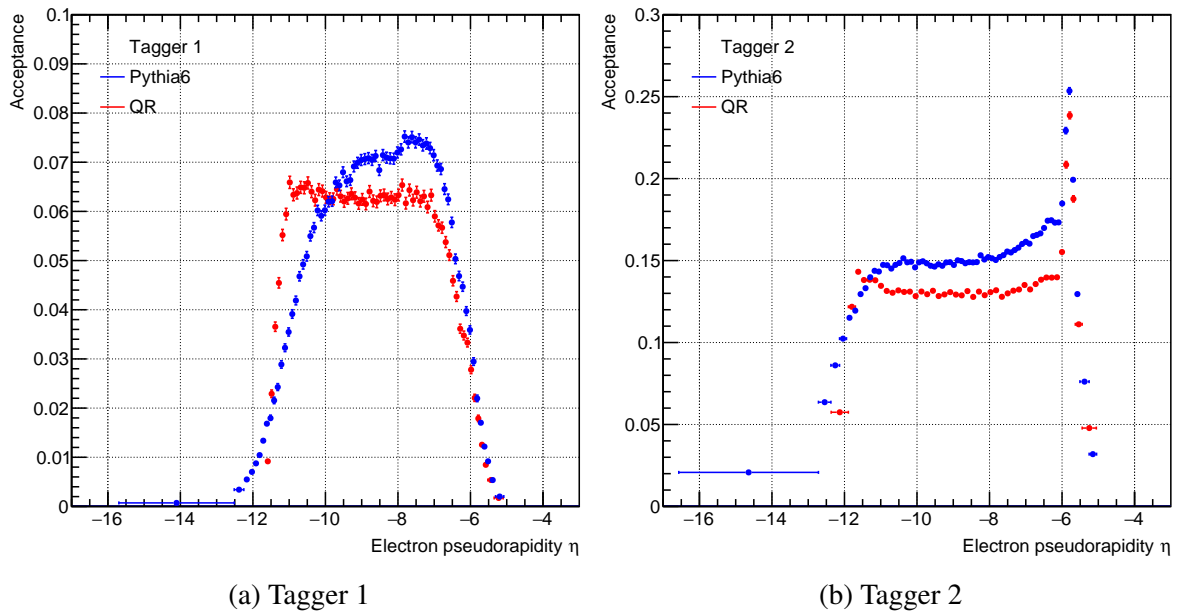


Fig. 17 Acceptance in electron pseudorapidity η for Tagger 1 (a) and Tagger 2 (b).

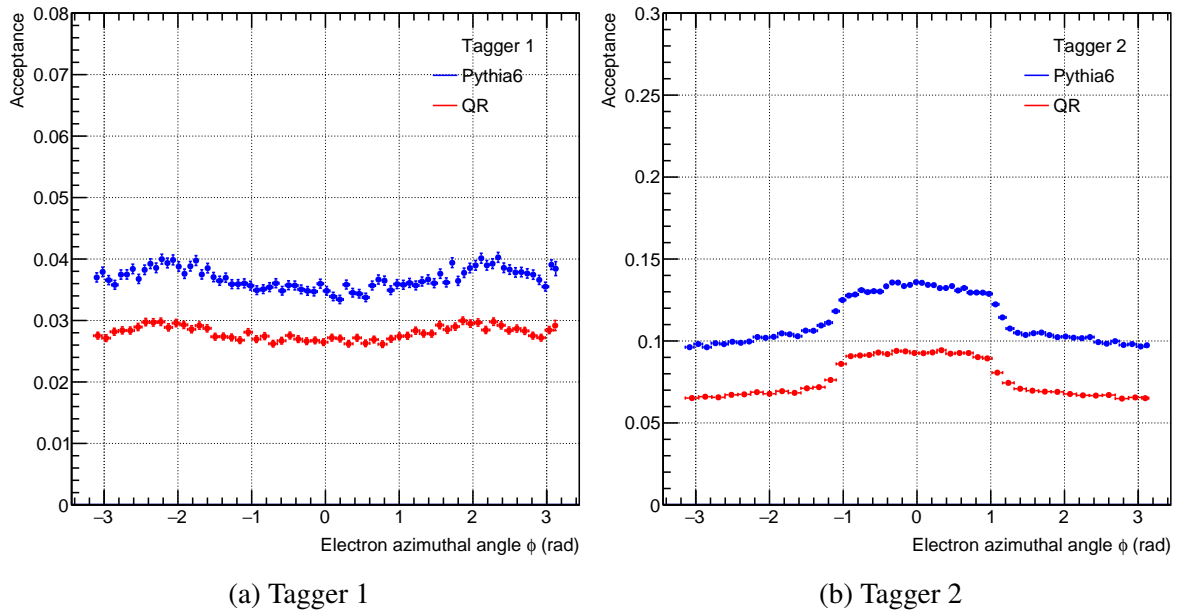


Fig. 18 Acceptance in electron azimuthal angle ϕ for Tagger 1 (a) and Tagger 2 (b).

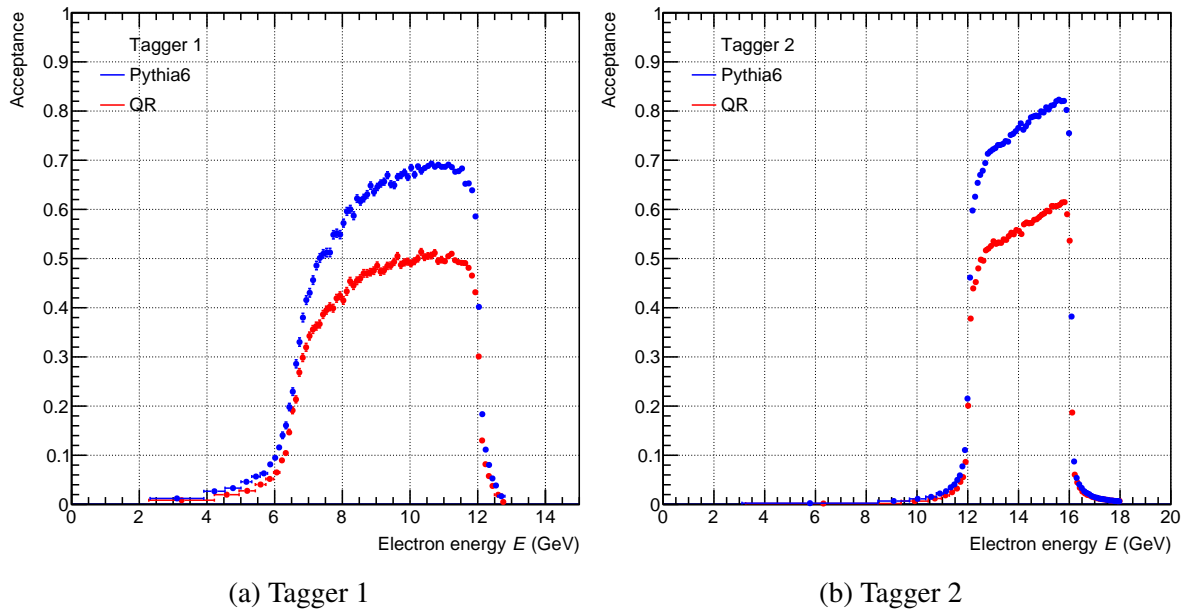


Fig. 19 Acceptance in electron energy E for Tagger 1 (a) and Tagger 2 (b).

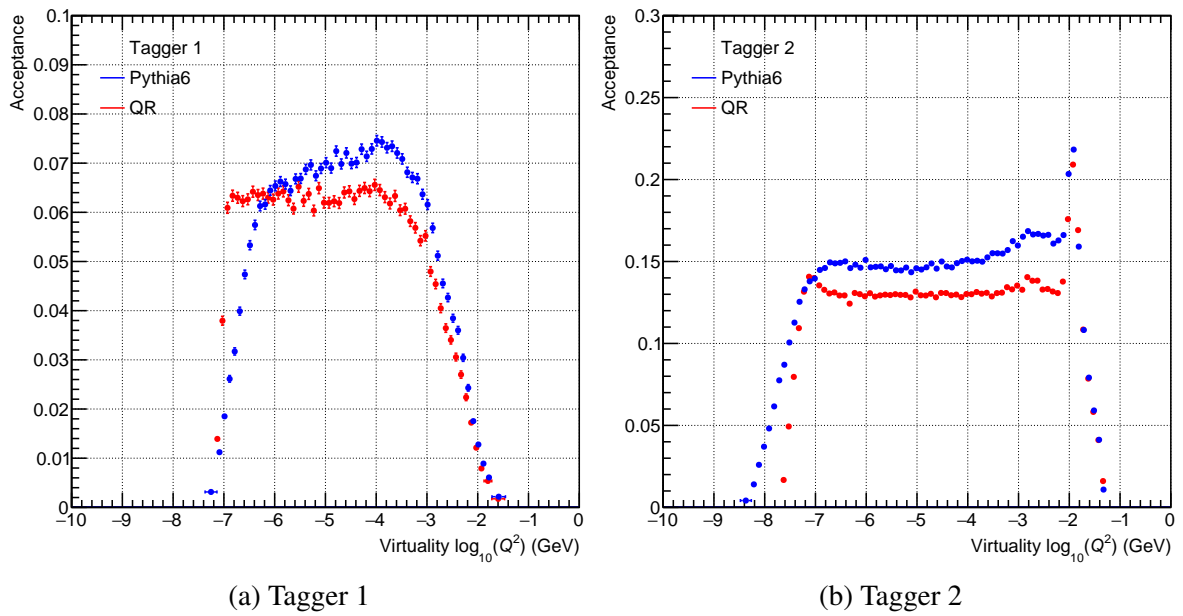


Fig. 20 Acceptance in Q^2 in terms of $\log_{10}(Q^2)$ for Tagger 1 (a) and Tagger 2 (b).

3.2 Acceptance in two variables

The acceptance is constructed in bins combining two variables. In each bin it is a ratio of events with a hit in one of the taggers to number of all generated events in that particular bin.

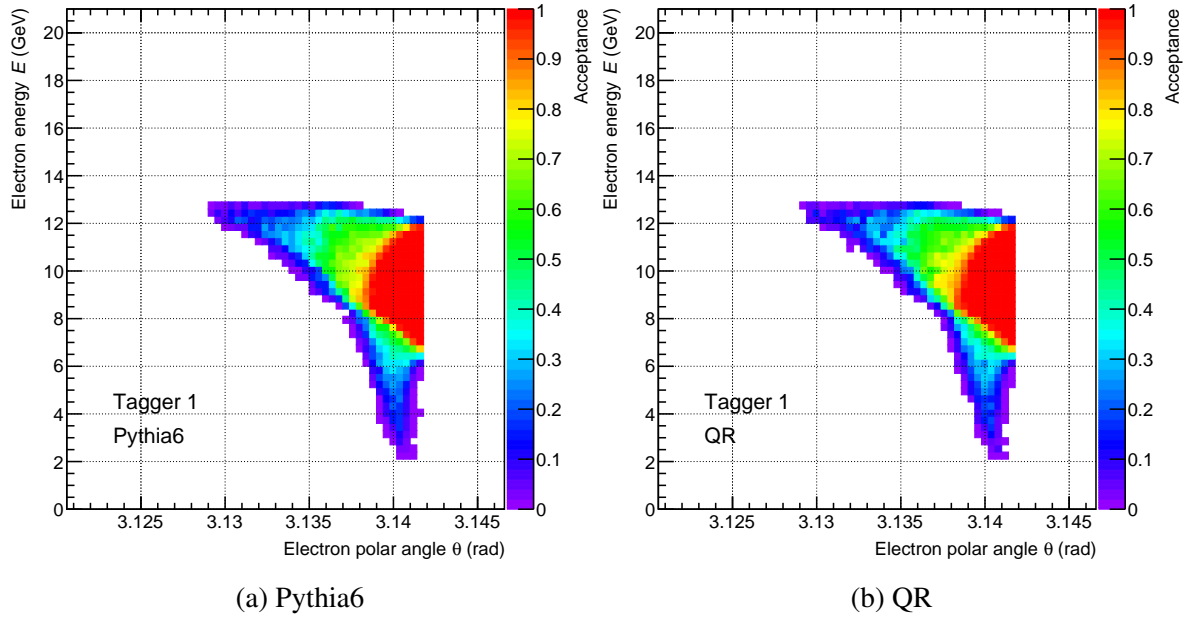


Fig. 21 Tagger 1 acceptance in E and θ for Pythia6 (a) and QR (b).

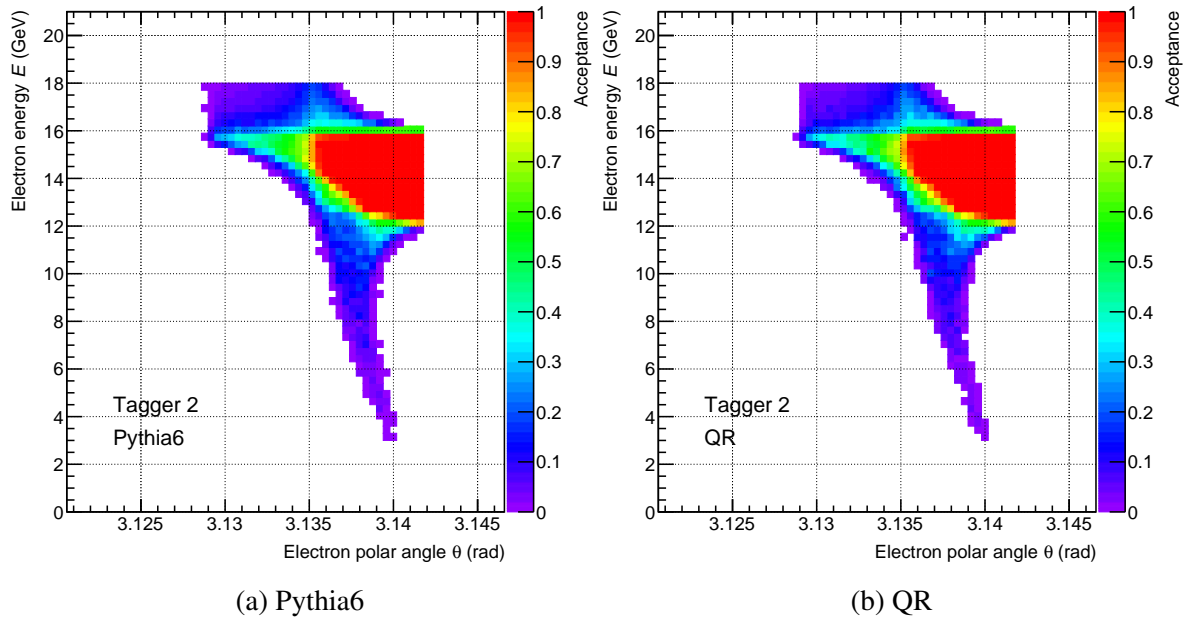


Fig. 22 Tagger 2 acceptance in E and θ for Pythia6 (a) and QR (b).

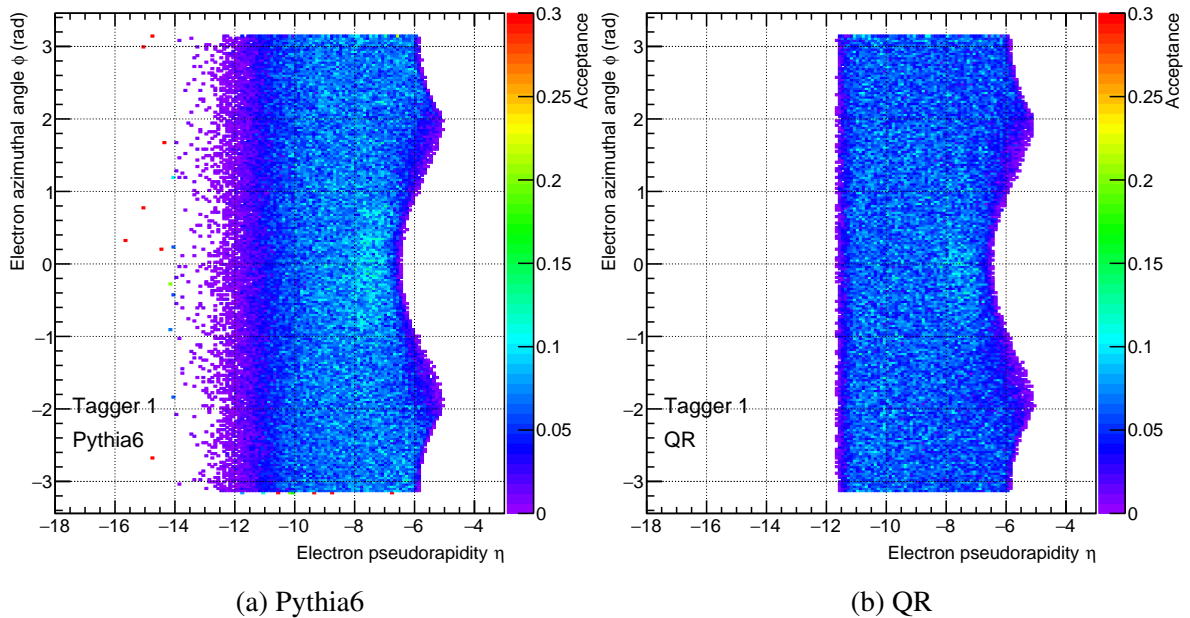


Fig. 23 Tagger 1 acceptance in ϕ and η for Pythia6 (a) and QR (b).

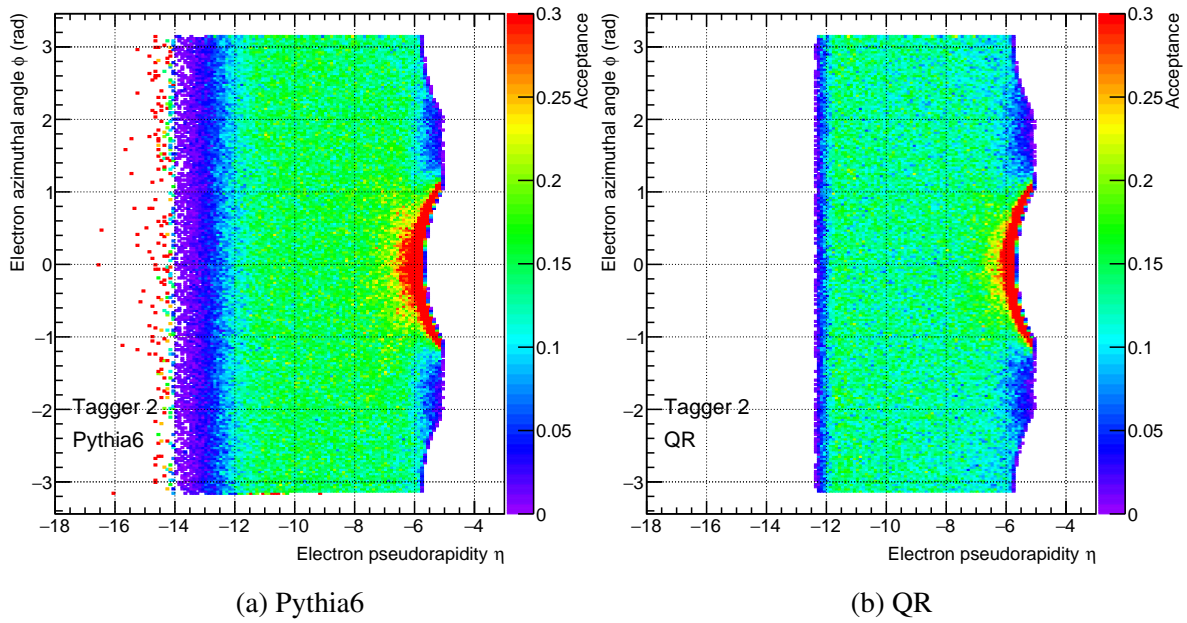


Fig. 24 Tagger 2 acceptance in ϕ and η for Pythia6 (a) and QR (b).

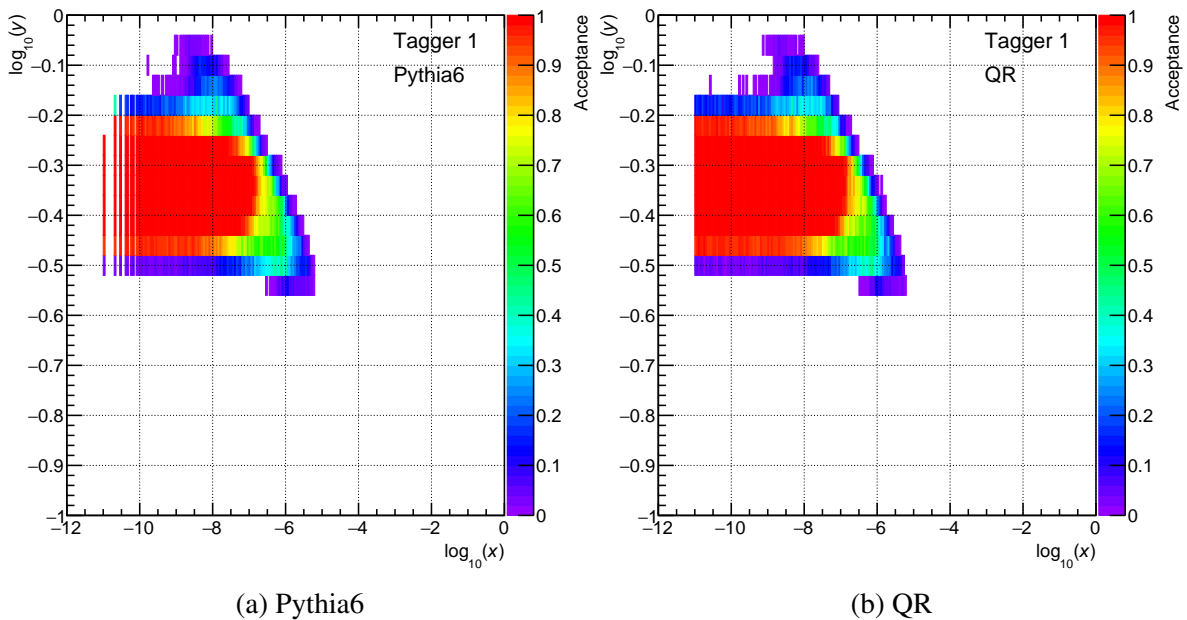


Fig. 25 Tagger 1 acceptance in inelasticity y and Bjorken- x for Pythia6 (a) and QR (b).

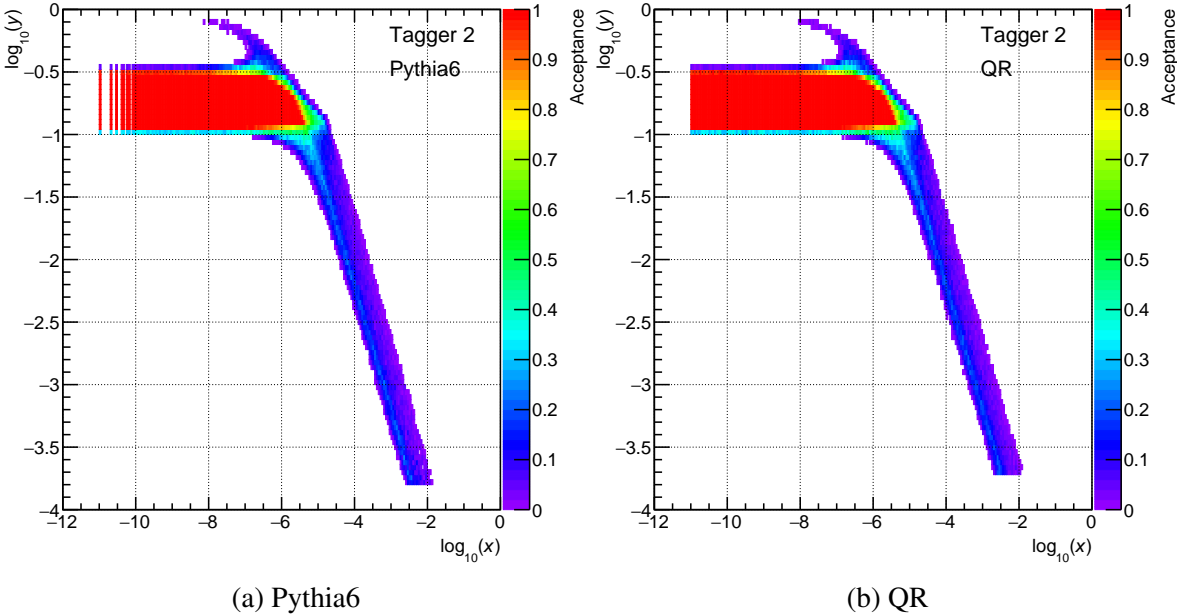


Fig. 26 Tagger 2 acceptance in inelasticity y and Bjorken- x for Pythia6 (a) and QR (b).

4 Summary

Acceptance of the two proposed tagger detectors has been shown as a function of several kinematics variables. The results are consistent among the two event generators used for this study.

Effect of angular divergence to kinematics of scattered electrons was briefly discussed. Polar angle is slightly affected at angles close to electron beam. A modulation is introduced to distribution of azimuthal angles. More pronounced effect is seen at large negative pseudo-rapidity.

Both taggers show compatible interval in Q^2 , within 10^{-7} to 10^{-2} GeV², although it is achieved at different range of electron energies. Behavior of acceptance is more complex in the case of Tagger 2, placed further from the interaction point.

A Generator steering cards

A.1 Pythia6 card

```

pythia.ep.18x275.5 Mevents.1.RadCor=0.Q2.all.txt ! output file name
11 ! lepton beam type
275, 18 ! proton and electron beam energy
50000,100 ! Number of events
1e-09, 0.99 ! xmin and xmax
1e-09,1.00 ! ymin and ymax
1e-09 , 200 ! Q2min and Q2max
F2PY,1998 ! F2-Model, R-Parametrisation
0 ! switch for rad corrections; 0:no, 1:yes, 2:gen.lookup table
1 ! Pythia-Model = 0 standard GVMD generation in Pythia-x and Q2; = 1 GVMD model
! with generation in y and Q2 as for radgen
1,1 ! A-Tar and Z-Tar
1,1 ! nuclear pdf parameter1: nucleon mass number A, charge number Z
201 ! nuclear pdf parameter2: correction order x*100+y x= 1:LO, 2:NLO y:error set
! PMAS(4,1)=1.27 ! charm mass
MSEL=2
!MSEL=0
!MSUB(91)=1
!MSUB(92)=1
!MSUB(93)=1
!MSUB(94)=1
!MSUB(95)=1
!MSUB(99)=1
!MSUB(131)=1
!MSUB(132)=1
!MSUB(135)=1
!MSUB(136)=1
!MSUB(11)=1
!MSUB(12)=1
!MSUB(13)=1
!MSUB(28)=1
!MSUB(53)=1
!MSUB(68)=1
MSTP(14)=30
MSTP(15)=0
MSTP(16)=1
MSTP(17)=4 ! MSTP 17=6 is the R-rho measured as by hermes, =4 Default
MSTP(18)=3
MSTP(19)=1 ! Hermes MSTP-19=1 different Q2 suppression, default = 4
MSTP(20)=0 ! Hermes MSTP(20)=0, default MSTP(20)=3
MSTP(32)=8
MSTP(38)=4
!MSTP(51)=10150 ! if pdflib is linked than non pythia-pdfs are available, like MSTP(51)=4046
MSTP(51)=7
MSTP(52)=1 ! ----> pdflib used MSTP 52=2
MSTP(53)=3
MSTP(54)=1
MSTP(55)=5
MSTP(56)=1
MSTP(57)=1
MSTP(58)=5
MSTP(59)=1
MSTP(60)=7
MSTP(61)=2
MSTP(71)=1
MSTP(81)=0
MSTP(82)=1
MSTP(91)=1
MSTP(92)=3 ! hermes MSTP(92)=4
MSTP(93)=1

```

```
MSTP(101)=3
MSTP(102)=1
MSTP(111)=1
MSTP(121)=0
! ----- Now all the PARPs -----
PARP(13)=1
PARP(18)=0.40 ! hermes PARP(18)=0.17
PARP(81)=1.9
PARP(89)=1800
PARP(90)=0.16
PARP(91)=0.40
PARP(93)=5.
PARP(99)=0.40
PARP(100)=5
PARP(102)=0.28
PARP(103)=1.0
PARP(104)=0.8
PARP(111)=2.
PARP(161)=3.00
PARP(162)=24.6
PARP(163)=18.8
PARP(164)=11.5
PARP(165)=0.47679
PARP(166)=0.67597 ! PARP165/166 are linked to MSTP17 as R_rho of HERMES is used
! PARP(166)=0.5
! ----- Now come all the switches for Jetset -----
PARJ(1)=0.100
PARJ(2)=0.300
PARJ(11)=0.5
PARJ(12)=0.6
PARJ(21)= 0.40
PARJ(32)=1.0
PARJ(33)= 0.80
PARJ(41)= 0.30
PARJ(42)= 0.58
PARJ(45)= 0.5
! -----
MSTJ(1)=1
MSTJ(12)=1
MSTJ(45)=5
MSTU(16)=2
MSTU(112)=5
MSTU(113)=5
MSTU(114)=5
! ----- Now all the CKINs for pythia -----
CKIN(1)=1.
CKIN(2)=-1.
CKIN(3)=0.
CKIN(4)=-1.
CKIN(5)=1.00
CKIN(6)=1.00
CKIN(7)=-10.
CKIN(8)=10.
CKIN(9)=-40.
CKIN(10)=40.
CKIN(11)=-40.
CKIN(12)=40.
CKIN(13)=-40.
CKIN(14)=40.
CKIN(15)=-40.
CKIN(16)=40.
CKIN(17)=-1.
CKIN(18)=1.
CKIN(19)=-1.
CKIN(20)=1.
CKIN(21)=0.
```

```
CKIN(22)=1.
CKIN(23)=0.
CKIN(24)=1.
CKIN(25)=-1.
CKIN(26)=1.
CKIN(27)=-1.
CKIN(28)=1.
CKIN(31)=2.
CKIN(32)=-1.
CKIN(35)=0.
CKIN(36)=-1
CKIN(37)=0.
CKIN(38)=-1.
CKIN(39)=4.
CKIN(40)=-1.
CKIN(65)=1.e-09      ! Min for Q^2
CKIN(66)=-1.        ! Max for Q^2
CKIN(67)=0.
CKIN(68)=-1.
CKIN(77)=2.0
CKIN(78)=-1.
```

A.2 Quasi-real card

```
[main]
```

```
Ee = 18 ; energy of electron beam, GeV
Ep = 275 ; proton beam, GeV
```

```
#range in x
xmin = 1e-11
xmax = 1
```

```
#range in y
ymin = 1e-4
ymax = 0.99
```

```
#minimal W, GeV
Wmin = 2
```

```
#range in Q^2
Q2min = 1e-9
Q2max = 1e7
```

```
#select the quasi-real parametrization
model = "quasi-real"
```

```
#number of events to generate
nev = 5000000
```

```
#output file name
nam = "qr_18x275_Qe_beff2_5Mevt"
```

```
[beam_effects]
```

```
#beam effects of angular divergence and emittance
```

```
use_beam_effects = true ; apply beam effects, true or false
```

```
theta_x = 163e-6 ; angular divergence in x, rad
theta_y = 202e-6 ; angular divergence in y, rad
```

```
sig_x = 0.236 ; vertex spread in x, mm
sig_y = 0.0162 ; vertex spread in y, mm
sig_z = 17.0 ; vertex spread in z, mm
```

B Steering cards for lmon geometry

B.1 Top geometry

```
#beamline
include ../config/geom_beamline.in

#low Q^2 taggers
include ../config/geom_lowQ2.in

#common top volume
new top topmain

    topmain.xsiz = 5000 # mm
    topmain.ysiz = 5000 # mm
    topmain.zsiz = 100000 # mm
```

B.2 Tagger detectors geometry

```
# geom_lowQ2.in :

# Tagger 1
new BoxCalV2 lowQ2s1

    lowQ2s1.zpos = -24000 # mm, position of front face in z
    lowQ2s1.xpos = 528.56 # mm, front face in x
    lowQ2s1.xsiz = 400 # mm, tagger size in x
    lowQ2s1.ysiz = 400 # mm, tagger size in y
    lowQ2s1.rot_y = -0.018332 # rad, rotation in x-z plane by rotation along y

# Tagger 2
new BoxCalV2 lowQ2s2

    lowQ2s2.zpos = -37000 # mm, position of front face in z
    lowQ2s2.xpos = 661.88 # mm, front face in x
    lowQ2s2.xsiz = 300 # mm, tagger size in x
    lowQ2s2.ysiz = 200 # mm, tagger size in y
    lowQ2s2.rot_y = -0.018332 # rad, rotation in x-z plane by rotation along y
```

B.3 Beamline layout

```
# geom_beamline.in :

new BeamMagnetV2 B2eR # B2eR beam dipole

    B2eR.zpos = -12250 # mm, center of the magnet along z
    B2eR.field = -0.200125 # tesla
    B2eR.length = 5500 # mm, total length along z
    B2eR.r1 = 97 # mm, entrance radius
    B2eR.r2 = 139 # mm, exit radius
    B2eR.rout = 200 # mm, vessel outer radius

new BoxCalV2 Q3eR # marker at Q3eR location

    Q3eR.zpos = -37995.904 # mm
    Q3eR.xpos = 472.033 # mm
    Q3eR.rot_y = -0.018332 # rad
    Q3eR.zsiz = 1
    Q3eR.xsiz = 700 # mm
    Q3eR.ysiz = 700 # mm
    Q3eR.vis_full = 0
```

```
new BeamQuadrupole Q1eR # Q1eR quadrupole

Q1eR.zpos = -6200 # mm
Q1eR.length = 1800 # mm
Q1eR.r1 = 66 # mm
Q1eR.r2 = 79 # mm
Q1eR.grad = 13.428092 # T/m

new BeamQuadrupole Q2eR # Q2eR quadrupole

Q2eR.zpos = -8300 # mm
Q2eR.length = 1400 # mm
Q2eR.r1 = 83 # mm
Q2eR.r2 = 94 # mm
Q2eR.grad = -12.850280 # T/m

new ConeAperture beampipe # beam aperture in front of quadrupole magnets

beampipe.zpos = -3480 # mm, front face of the cone along z
beampipe.length = 1817 # mm, cone length
beampipe.r1 = 80 # mm, inner radius closer to the IP
beampipe.r2 = 66 # mm, inner radius further from the IP
beampipe.dr = 2 # mm, cone radial thickness

new ConeAperture central_beampipe # beam pipe in front of ecal

central_beampipe.zpos = 0 # mm
central_beampipe.length = 3480
central_beampipe.r1 = 66
central_beampipe.r2 = 66
central_beampipe.dr = 2

new ConeAperture rear_beampipe # beam after B2eR

rear_beampipe.zpos = -15010 # mm, entrance position in z
rear_beampipe.xpos = 50.42 # mm, entrance position in x
rear_beampipe.length = 22980 # total length
rear_beampipe.angle = -0.018332 # rad
rear_beampipe.r1 = 139 # mm, B2eR exit radius
rear_beampipe.r2 = 40 # mm, Q3eR entrance radius
rear_beampipe.dr = 2 # mm, vessel thickness
rear_beampipe.transparent = 1 # transparent for particles
```